A conserved CaM- and radial spoke–associated complex mediates regulation of flagellar dynein activity

Erin E. Dymek and Elizabeth F. Smith

Department of Biological Sciences, Dartmouth College, Hanover, NH 03755

For virtually all cilia and eukaryotic flagella, the second messengers calcium and cyclic adenosine monophosphate are implicated in modulating dynein-driven microtubule sliding to regulate beating. Calmodulin (CaM) localizes to the axoneme and is a key calcium sensor involved in regulating motility. Using immunoprecipitation and mass spectrometry, we identify members of a CaM-containing complex that are involved in regulating dynein activity. This complex includes flagellar-associated protein 91 (FAP91), which shares considerable sequence similarity to AAT-1, a protein originally identified in testis as an A-kinase anchor protein (AKAP)–binding protein. FAP91 directly interacts with radial spoke protein 3 (an AKAP), which is located at the base of the spoke. In a microtubule sliding assay, the addition of antibodies generated against FAP91 to mutant axonemes with reduced dynein activity restores dynein activity to wild-type levels. These combined results indicate that the CaM- and spoke-associated complex mediates regulatory signals between the radial spokes and dynein arms.

Introduction

For eukaryotic cells that use cilia and flagella for motile functions, motility is commonly modulated in response to extracellular cues; this modulation may include changes in waveform (Brokaw et al., 1974; Brokaw, 1979; Bessen et al., 1980; Kamiya and Witman, 1984), beat frequency (Verdugo, 1980), or direction of the effective stroke (Naitoh and Kaneko, 1972; Izumi and Miki-Noumura, 1985). Despite the diversity of responses between cell types, changes in motility are often preceded and mediated by changes in the intraflagellar concentrations of the second messengers calcium and cAMP. Ciliary and flagellar beating results from the spatial regulation of dynein activity along the axonemal microtubules (Satir, 1985). Our goal is to understand how changes in intraflagellar calcium concentrations are converted to changes in dynein-driven microtubule sliding to modulate motility.

Substantial evidence from our laboratory and others indicates that the central apparatus and radial spokes form a signal transduction pathway that modulates ciliary and flagellar beating in response to second messengers (for reviews see Porter and Sale, 2000; Smith and Yang, 2004). Using both functional and structural approaches, our previous studies demonstrated that calcium control of motility involves the regulation of dynein-driven microtubule sliding and that CaM is a key axonemal calcium sensor (Smith, 2002a,b; Wargo and Smith, 2003; Wargo et al., 2004). Based on these results, we postulate that the calcium sensor regulates the activity of specific dynein subforms and/or dynein arms attached to specific subsets of doublet microtubules, thus modulating the size and shape of ciliary/flagellar bends.

Understanding how CaM might regulate dynein activity to modulate ciliary motility requires the localization of CaM within the axoneme as well as the identification of CaM binding partners. Yang et al. (2001) have reported that a fraction but not all of the axonemal CaM associates with the radial spokes in *Chlamydomonas reinhardtii*. We have identified and characterized additional CaM-binding proteins in *C. reinhardtii* flagella using an immunoprecipitation approach. We developed antibodies against a peptide antigen unique to the C terminus of *C. reinhardtii* CaM and used these antibodies to precipitate CaM from extracted axonemal proteins. We previously reported that eight polypeptides precipitate with CaM and that these polypeptides form at least two different protein complexes (Wargo et al., 2005). One complex is comprised of five polypeptides in addition to CaM and is associated with the C1 microtubule of the

Correspondence to Elizabeth F. Smith: elizabeth.f.smith@dartmouth.edu

Abbreviations used in this paper: AKAP, A-kinase anchor protein; CSC, CaM- and spoke-associated complex; DRC, dynein regulatory complex; EST, expressed sequence tag; FAP, flagellar-associated protein; RSP, radial spoke protein.

The online version of this article contains supplemental material.

The Journal of Cell Biology, Vol. 179, No. 3, November 5, 2007 515–526
http://www.jcb.org/cgi/doi/10.1083/jcb.200703107

axonemal central apparatus (Wargo et al., 2005). Here, we report the identities and localization of three polypeptides comprising the second CaM-containing complex and provide data supporting the hypothesis that this complex plays an important role in modulating the activity of specific subsets of dynein arms.

Results

CaM immunoprecipitation and peptide identification

To identify CaM-containing complexes within the axoneme, we used anti-CaM antibodies in immunoprecipitation experiments (Wargo et al., 2005). Using extracts isolated from mutant axonemes lacking the radial spokes (*pf14*), our anti-CaM antibodies precipitated a total of eight polypeptides in addition to CaM (Fig. 1; see Fig. 4 a in Wargo et al., 2005). Five polypeptides form a complex that includes PF6 and localizes to the C1a projection of the central apparatus (Wargo et al., 2005). However, the three additional polypeptides that are precipitated (designated CaM-IP2, -IP3, and -IP4; Fig. 1) are present in all central apparatus–defective mutants, including *pf6*. Therefore, these three polypeptides are not components of the radial spokes or central apparatus. These three polypeptides are also precipitated from extracts isolated from mutant axonemes lacking the outer dynein arms and inner arm I1 (*pf28pf30*; Fig. 1) as well as the inner arm–defective strains *mia1* and *mia2* (not depicted), indicating that they do not localize to these dynein subforms. All three polypeptides are also precipitated from the move backward–only strains *mbo1* and *mbo2* (unpublished data), indicating that the assembly of these polypeptides is unaffected in these mutant strains.

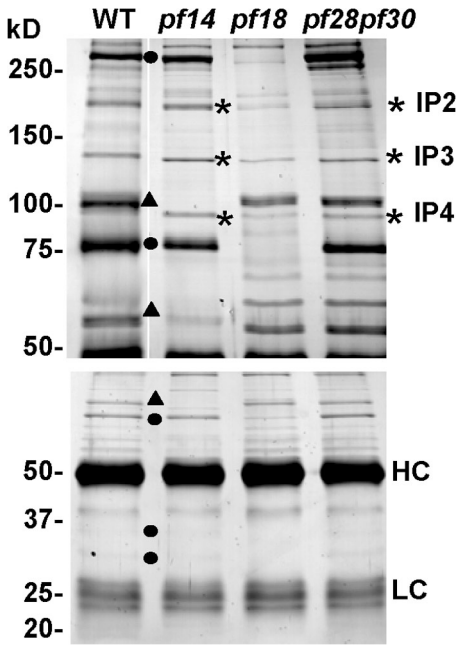

Figure 1. **Silver-stained gels of immunoprecipitation experiments using anti-CaM antibodies and extracts isolated from wild-type, radial spokeless (*pf14*), and central pairless (*pf18*) axonemes as well as axonemes lacking both the outer dynein arms and inner arm isoform I1 (*pf28pf30*).** The precipitates were resolved on either a 7% (top) or 12% (bottom) acrylamide gel. Central apparatus proteins are indicated by dots; spoke proteins are indicated by triangles. CaM-IP2, -IP3, and -IP4 are indicated by asterisks. The darkly stained bands are the heavy (HC) and light (LC) chains from the antibodies. CaM-IP2, -IP3, and -IP4 are precipitated from all of the mutant extracts tested, indicating that these polypeptides are not components of the radial spokes, central apparatus, outer dynein arms, or inner dynein arm I1.

To determine the identities of CaM-IP2, -IP3, and -IP4, these polypeptides were excised from gels and analyzed by mass spectrometry (see Materials and methods; data summarized in Table I). The identity of CaM-IP2 was determined from four peptide sequences. Based on searches of the *C. reinhardtii* genome database (version 3.0; http://genome.jgi-psf.org/Chlre3/Chlre3.home.html), the *CaM-IP2* gene is located on the same contig as Zsp1; therefore, the *CaM-IP2* gene is most likely on linkage group VII. In searches of the *C. reinhardtii* proteome database, CaM-IP2 is flagellar-associated protein 91 (FAP91; Pazour et al., 2005). BLAST searches reveal that CaM-IP2 (FAP91) is most similar to the human homologue of AAT-1 (C3orf15; GenBank/EMBL/DDBJ accession no. AAH35238; E value of E = 7e-49). AAT-1 was originally identified as a testis-specific protein in mice that forms a quaternary complex with AMY-1 (a c-myc–binding protein), an A-kinase anchoring protein (AKAP), and two regulatory subunits of PKA (cAMP-dependent protein kinase; Yukitake et al., 2002). More recently, a total of seven alternatively spliced isoforms of AAT-1 have been identified, and some of these isoforms are expressed in a variety of human tissues (Matsuda et al., 2005). The largest isoform of AAT-1, AAT-1L, is an ∼90-kD protein. The testis-specific isoform AAT-1α is reported to contain only the C-terminal 98 amino acids of AAT-1L.

CaM-IP2 is 32% identical and 49% similar to AAT-1 over a stretch of 423 amino acids at the N terminus (Fig. S1, available at http://www.jcb.org/cgi/content/full/jcb.200703107/DC1). Sequence similarity with AAT-1 may extend beyond the N terminus of the protein, but the C-terminal half of the CAM-IP2 sequence is not represented in the *C. reinhardtii* genome. We have tried to complete the CaM-IP2 coding sequence using a variety of approaches, including 5′ and 3′ rapid amplification of cDNA ends, obtaining small genomic fragments of CaM-IP2 for sequencing, and optimizing our sequencing reactions for GC-rich sequences. We have confirmed the predicted amino acid sequence for the N-terminal one third of the protein but were unsuccessful in obtaining the complete coding sequence. As judged by SDS-PAGE, the apparent molecular mass of CaM-IP2 is 183 kD, which is almost double that of AAT-1L. However, Northern blots of RNA isolated from wild-type cells indicate that the CaM-IP2 transcript is ∼4.4 kb (Fig. S2). Based on our experience comparing *C. reinhardtii* genomic and coding sequences, the true molecular weight of this protein is most likely no greater than 120 kD.

The identity of CaM-IP3 was determined from the amino acid sequence of five peptides. Based on database searches, CaM-IP3 is located on linkage group III and corresponds to FAP61. Using corresponding cDNA sequences in the *C. reinhardtii* expressed sequence tag (EST) database and RT-PCR, we determined that the *CaM-IP3* gene encodes a 1,115–amino acid protein that contains a predicted NADH dehydrogenase domain. This domain is found in both class I and II oxidoreductases as well

Table I. **Proteins precipitated with anti-CaM antibodies**

Name	Predicted molecular mass	Apparent molecular mass	pI	Similarities	Flagellar proteome	Linkage group
CaM-IP2	ND	183 kD	ND	AAT-1, AKAP-binding protein	FAP91	VII
CaM-IP3	118 kD	140 kD	4.8	pyridine-disulfide oxidoreductase domain	FAP61	III
CaM-IP4	97 kD	100 kD	7.4	WD repeats	FAP251	III

as NADH oxidases and peroxidases. The domain includes a small NADH-binding domain within a flavin adenine dinucleotide–binding domain and, thus, is thought to be involved in energy conversion. Searches of sequence databases reveal that the predicted human protein C20orf26 is most similar to CaM-IP3 (E value of E = 6.8e-56), sharing 25% identity and 43% amino acid similarity along the entire length of the protein. The predicted molecular mass of CaM-IP3 is 118 kD, although the protein has an apparent molecular mass of ~140 kD as judged by SDS-PAGE. The acidic isoelectric point of CaM-IP3 (4.76) may partially account for this discrepancy.

The identity of CaM-IP4 was determined from the amino acid sequence of five peptides. Based on database searches, CaM-IP4 is also located on linkage group III and corresponds to FAP251. CaM-IP4 contains seven WD-40 repeats that comprise much of the N terminus of the protein. WD-40 repeats form propeller-like structures that serve as an interface for protein–protein interactions (Neer et al., 1994). In searches of sequence databases, a protein predicted from the *Leishmania* database (GenBank/EMBL/DDBJ accession no. XM811714; E value of E = 9e-53) is most similar to CaM-IP4 with 29% amino acid identity and 43% similarity along the entire length of this protein. CaM-IP4 is also 24% similar and 39% identical to a protein predicted from the human genome sequence (GenBank/EMBL/DDBJ accession no. BC036233; E value of E = 6e-37). All of these polypeptides show similarity to microtubule-associated protein–like 5 from echinoderms. In addition to the WD-40 repeats, each of these proteins has a putative EF-hand domain at the C terminus. Although a motifs search does not predict an EF hand at the C terminus of CaM-IP4, the InterProScan algorithm provided by the European Molecular Biology Laboratory predicts an EF hand–like domain.

CaM-IP2, -IP3, and -IP4 form a single complex

Based on CaM immunoprecipitation, it is possible that CaM-IP2, -IP3, and -IP4 bind CaM individually, in subsets, or together to form a single complex. To differentiate among these possibilities, we developed polyclonal antibodies in rabbits against either bacterially expressed protein fragments or synthetic peptides for each of CaM-IP2, -IP3, and -IP4 (see Materials and methods). CaM-IP4 proved to be nonantigenic. However, we were successful in obtaining antibodies that specifically recognize either CaM-IP2 or CaM-IP3 on Western blots (Fig. 2 A).

We then used these antibodies in immunoprecipitation experiments. Antibodies generated against CaM-IP3 failed to precipitate CaM-IP3. On the other hand, the CaM-IP2 antibody specifically precipitated CaM-IP2 as well as -IP3 and -IP4 from extracts isolated from radial spokeless axonemes (Fig. 2 B, middle lane). For extracts isolated from wild-type and *pf18* axonemes, additional polypeptides are precipitated by the CaM-IP2 antibodies that are not precipitated from extracts of the spokeless mutant *pf14*. Based on the molecular weights of these polypeptides (Yang et al., 2001) as well as their absence from precipitates of *pf14* axonemal extracts, we suspected that these polypeptides were radial spoke components. Corresponding Western blots using antibodies generated against radial spoke protein 2 (RSP2) and RSP3 confirm that RSPs are precipitated by the CaM-IP2 antibodies. The simplest interpretation of these

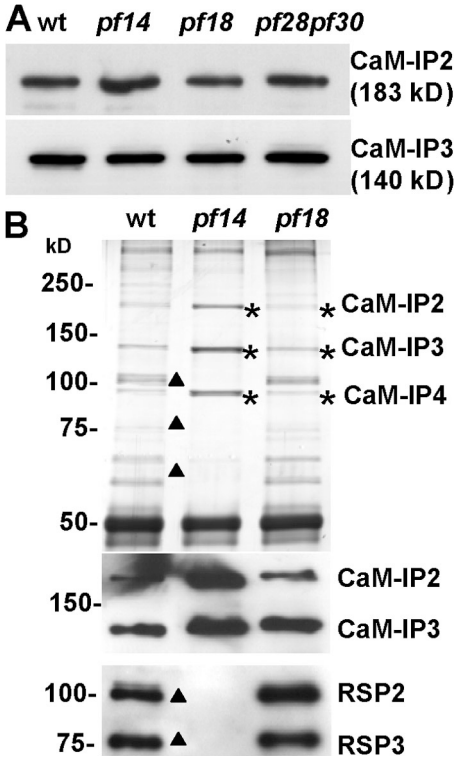

Figure 2. **CaM-IP2, -IP3, and -IP4 form a single complex that is associated with the radial spokes.** (A) Western blots of axonemes (8 μg per lane) probed with antibodies generated against CaM-IP2 and -IP3. Both polypeptides are present in all axonemes in approximately equal amounts. (B) Silver-stained gel (top) and corresponding Western blots (middle and bottom) of immunoprecipitation experiments using anti–CaM-IP2 antibodies and wild-type, radial spokeless (*pf14*), and central pairless (*pf18*) axonemal extracts. CaM-IP2 antibodies precipitate the CaM-IP2, -IP3, and -IP4 complex (asterisks) as well as RSPs (triangles). Blots were probed with antibodies generated against CaM-IP2, -IP3, RSP2, or RSP3. These results indicate that CaM-IP2, -IP3, and -IP4 form a single complex that is associated with the radial spokes.

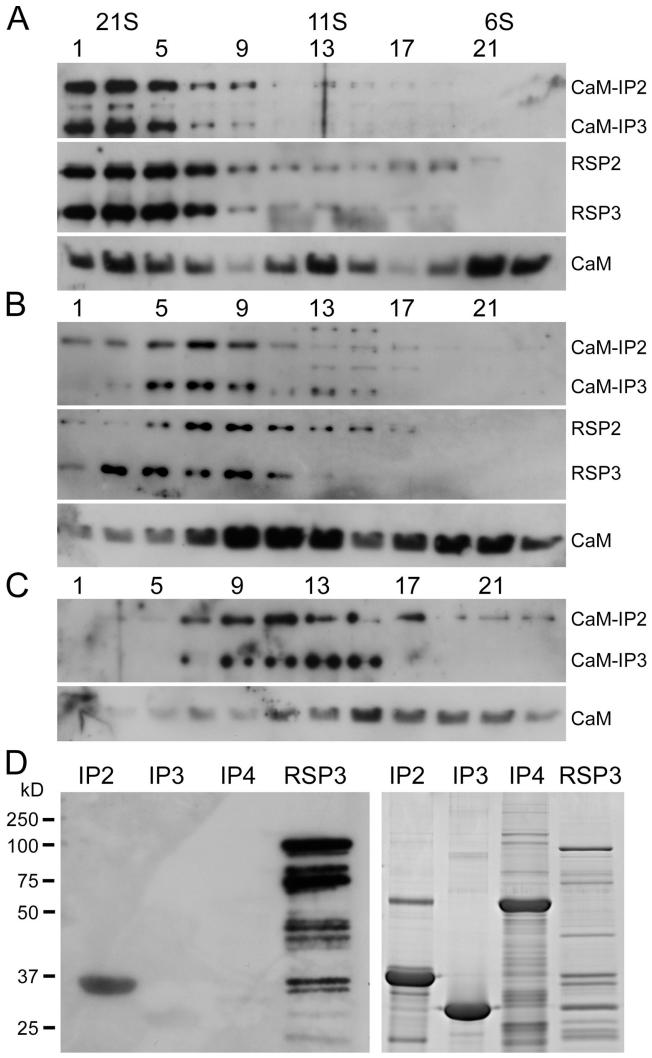

Figure 3. **CaM-IP2 is associated with RSP3.** Western blots of extracts isolated from wild-type (A), spoke headless (B; *pf17*), and spokeless (C; *pf14*) axonemes fractionated on sucrose gradients. Blots were probed with antibodies generated against CaM-IP2, -IP3, RSP2, RSP3, or CaM. In extracts isolated from both wild-type or *pf17* axonemes, CaM-IP2 and -IP3 cosediment with spoke stalk components. In extracts isolated from both *pf17* and *pf14* mutant axonemes, the sedimentation value for the CaM-IP2 complex is considerably lower than that in wild type. (D) Gel overlay of expressed RSP3. Bacterial extracts expressing fragments of CaM-IP2 (37 kD), -IP3 (32 kD), -IP4 (60 kD), and RSP3-GST (110 kD) were resolved on polyacrylamide gels and either transferred to nitrocellulose (left) or stained with Coomassie blue (right). The membrane (left) was incubated with expressed RSP3 and probed with antibodies generated against RSP3. These results indicate that RSP3 binds to CaM-IP2.

results is that CaM and CaM-IP2, -IP3, and -IP4 form a single complex that is associated with the radial spokes.

CaM-IP2 binds to RSP3

To provide further evidence that the CaM-IP2, -IP3, and -IP4 complex is associated with the radial spokes, we investigated whether this complex cosediments with the radial spokes using sucrose density gradient centrifugation (Fig. 3). For axonemal extracts isolated from wild-type flagella, the polypeptides comprising the radial spokes cosediment at ~20S (Yang et al., 2001). Western blots of corresponding gradient fractions reveal that CaM-IP2 and -IP3 cosediment with the radial spokes. For axonemal extracts isolated from flagella that lack the spoke heads (*pf17*), the polypeptides comprising the spoke stalks cosediment at ~15S (Yang et al., 2001). Western blots of corresponding gradient fractions from *pf17* extracts reveal that CaM-IP2 and -IP3 also cosediment with the radial spoke stalks (Fig. 3 B). For axonemal extracts isolated from flagella that completely lack the radial spokes (*pf14*), CaM-IP2 and -IP3 cosediment as a smaller complex at ~11S (Fig. 3 C). Although we do not have antibodies that recognize CaM-IP4, immunoprecipitation experiments using sucrose gradient fractions confirm that CaM-IP4 also cosediments with CaM-IP2, -IP3, and -IP4 (Fig. S3, available at http://www.jcb.org/cgi/content/full/jcb.200703107/DC1). These results support the hypothesis that CaM, CaM-IP2, -IP3, and -IP4 form a single complex that is associated with the spoke stalk.

As noted in our CaM-IP2 sequence analysis, CaM-IP2 is most similar to AAT-1, which is thought to form a quaternary complex with an AKAP-binding protein. Based on previous reports that RSP3 is an AKAP (Gaillard et al., 2001), that RSP3 is located at the base of the radial spoke stalk (Diener et al., 1993), and our results that CaM-IP2 cosediments with the spoke stalk (this study), we hypothesized that CaM-IP2 binds to RSP3. To test this hypothesis, we used a gel overlay assay. Bacterially expressed proteins (CaM-IP2, CaM-IP3, and RSP3) were resolved by SDS-PAGE and transferred to nitrocellulose membrane. The membrane was then incubated with bacterially expressed *C. reinhardtii* RSP3, and the overlain protein was detected by immunoblotting. As shown in Fig. 3 D, RSP3 binds only to CaM-IP2. These combined results indicate that CaM-IP2, -IP3, and -IP4 are associated with the radial spoke stalk via interactions between CaM-IP2 and RSP3.

CaM binding is calcium sensitive

The association of CaM with specific proteins is regulated by the calcium-binding state of CaM. All immunoprecipitation experiments were performed using low calcium conditions. Therefore, the eight polypeptides we precipitated do not require calcium to form protein complexes with CaM. To investigate whether CaM binding of these polypeptides is calcium sensitive, we first immunoprecipitated CaM from *pf14* axonemal extracts under low calcium conditions; the protein A beads were then washed using high calcium buffer (see Materials and methods). CaM remained associated with the beads, whereas CaM-IP2, -IP3, and -IP4 were selectively extracted in the presence of high calcium (Fig. 4 A). These results demonstrate that the binding of CaM-IP2, -IP3, and -IP4 to CaM is calcium sensitive. We also performed immunoprecipitation experiments using the CaM-IP2 antibody under high calcium conditions. All three members of the complex are precipitated by the CaM-IP2 antibody in extracts from spokeless axonemes, indicating that the complex does not dissociate under high calcium conditions (Fig. 4 B). In addition, the CaM-IP2 antibodies precipitate the spokes from axonemal extracts isolated from either wild-type or central pairless axonemes, indicating that the complex does not dissociate from the spokes under high calcium conditions (Fig. 4 B).

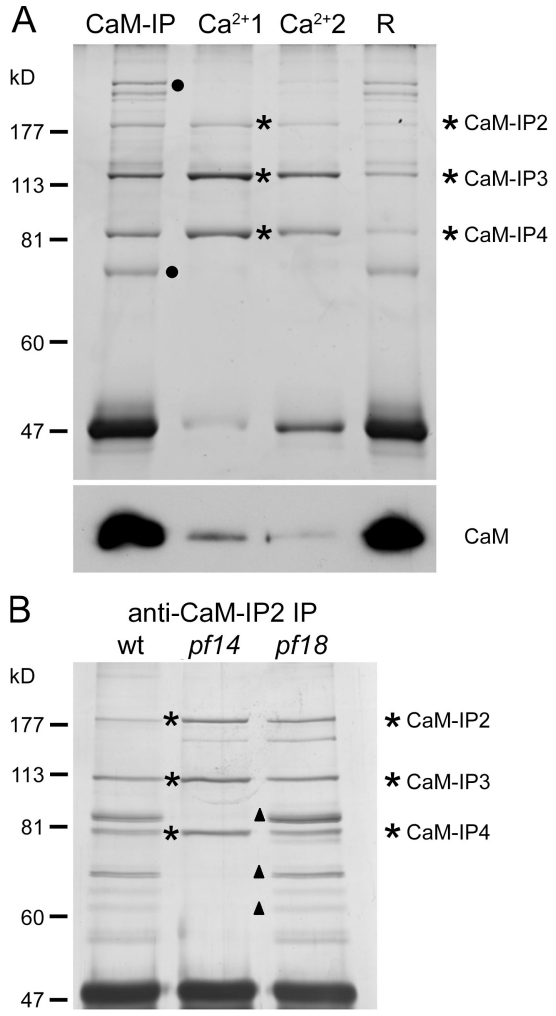

Figure 4. **Binding of CaM-IP2, -IP3, and -IP4 to CaM is calcium sensitive.** (A) Silver-stained gel of CaM immunoprecipitation from radial spokeless axonemal extracts (*pf14*) followed by treatment with $CaCl_2$ (top). After precipitation (CaM-IP), the protein A beads were washed twice with 2 mM $CaCl_2$ ($Ca^{2+}1$ and $Ca^{2+}2$), and the resulting extract was loaded onto the gel. Proteins remaining (lane R) associated with the beads after the $CaCl_2$ wash were eluted with sample buffer. CaM-IP2, -IP3, and -IP4 (asterisks) are extracted from the beads. In contrast, the central pair proteins (dots) are not extracted with $CaCl_2$. Western blots using anti-CaM antibodies (bottom) reveal that $CaCl_2$ extracts very little CaM from the beads. These results indicate that binding of CaM-IP2, -IP3, and -IP4 to CaM is calcium sensitive. (B) Silver-stained gel of immunoprecipitation experiments performed in 1 mM $CaCl_2$ using anti–CaM-IP2 antibodies and wild-type, spokeless (*pf14*), and central pairless (*pf18*) axonemal extracts. The CaM-IP2 antibodies precipitate the CaM-IP2, -IP3, and -IP4 complex (asterisks) and spokes (triangles), indicating that they do not dissociate from each other or the spokes in high calcium buffer conditions.

The association of CaM-IP2, -IP3, and -IP4 with CaM is altered in DRC mutants

Our data are consistent with the localization of a CaM-containing complex at the base of the spokes. Previous studies have indicated that the components of the dynein regulatory complex (DRC) localize to the doublet microtubules near the spokes (Piperno et al., 1992; Gardner et al., 1994; Nicastro et al., 2006). Therefore, we hypothesized that the CaM-IP2, -IP3, and -IP4 complex may be disrupted in mutants lacking subsets of DRC components. To investigate this possibility, we precipitated the complex from axonemal extracts isolated from DRC mutants (*pf2* and *pf3*) using either our anti-CaM or anti–CaM-IP2 antibodies. The anti-CaM antibodies precipitate substantially less CaM-IP2, -IP3, and -IP4 from *pf2* and *pf3* axonemal extracts compared with that precipitated from wild-type extracts even though axonemes isolated from these mutants appear to have wild-type levels of CaM as judged by Western blotting (Fig. 5). These results suggest that the assembly of CaM-IP2, -IP3, and -IP4 is defective in DRC mutants. However, when we precipitate the complex using our anti–CaM-IP2 antibodies, the precipitates from *pf2* and *pf3* are indistinguishable from that of wild type (Fig. 5). These results indicate that CaM-IP2, -IP3, and -IP4 assemble normally in DRC mutants but that their association with CaM is disrupted.

Anti–CaM-IP2 antibodies restore dynein activity to mutant axonemes

Localization of the CaM-IP2, -IP3, and -IP4 complex at the base of the radial spokes, potentially near DRC components, suggested a possible role in modulating dynein-driven microtubule sliding. Based on this localization, we hypothesized that regulation of dynein activity by this complex would occur downstream of regulatory signals derived from the radial spokes or central apparatus. To test this hypothesis, we conducted the microtubule sliding assay in the presence of the anti–CaM-IP2 antibody. We initially tested whether the antibodies possessed any function-blocking activity using wild-type axonemes and a microtubule sliding assay (see Materials and methods). The anti–CaM-IP2 antibodies had no effect on microtubule sliding velocity (Fig. 6 A).

We then examined dynein activity in mutant axonemes. The first mutant tested was the central pairless strain *pf18*; axonemes from this mutant have reduced dynein activity compared with wild-type (Smith, 2002b). To our surprise, the anti–CaM-IP2 antibody significantly increases microtubule sliding velocity ($P < 0.001$ by *t* test; Fig. 6 A). In addition, the increase in velocity in central pairless axonemes is dependent on the concentration of the antibody, with maximal effect at 0.2 μM CaM-IP2 antibody (Fig. 6 B). Importantly, the increase in dynein activity is not observed upon the addition of anti–CaM-IP3 or anti-C1a32 antibodies (Wargo et al., 2005), further indicating that the effect is specific for binding of the anti–CaM-IP2 antibody. Based on these results and the hypothesis that the complex affects dynein activity downstream of regulatory cues from the radial spokes, we predicted that addition of our antibodies to radial spokeless axonemes would also increase dynein activity. Indeed, addition of the CaM-IP2 antibodies to radial spokeless axonemes (*pf14*) significantly increases dynein activity ($P < 0.001$ by *t* test; Fig. 6 D). The simplest interpretation of these results is that the CaM-IP2, -IP3, and -IP4 complex is involved in modulating the activity of the dynein arms.

To determine whether specific subforms of axonemal dynein are the targets for modulation by this complex, we repeated the sliding microtubule experiments using mutants that lack specific dynein subforms. The CaM-IP2 antibodies have no effect on the sliding velocities of a mutant lacking the outer dynein arms (*pf28*; Fig. 6 C). Double mutants lacking both the

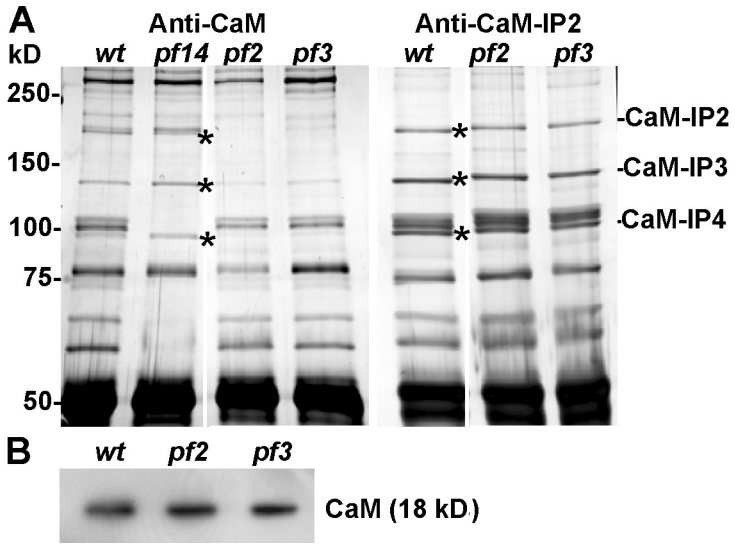

Figure 5. **Association of the CaM-IP2 complex with CaM is disrupted in DRC mutants.** (A) Silver-stained gel of immunoprecipitates using either anti-CaM or anti–CaM-IP2 antibodies and axonemal extracts isolated from wild-type (wt), spokeless (*pf14*), or DRC mutant (*pf2* and *pf3*) axonemes. Compared with wild-type and *pf14* precipitates, the CaM-IP2 complex is substantially reduced in precipitates of *pf2* and *pf3* extracts using the anti-CaM antibodies. However, immunoprecipitation using the anti–CaM-IP2 antibodies indicates that relatively equal amounts of CaM-IP2, -IP3, and -IP4 (asterisks) are precipitated in wild-type, *pf2*, and *pf3* axonemes. (B) Western blot of isolated axonemes using anti-CaM antibodies. The *pf2* and *pf3* mutant axonemes have wild-type levels of CaM. These combined results indicate that association of the CaM-IP2 complex with CaM is disrupted in DRC mutants.

central apparatus and outer dynein arms (*pf18pf28*) or radial spokes and outer dynein arms (*pf14pf28*) have shorter length flagella than wild type, and many of the isolated axonemes fail to undergo microtubule sliding in this assay. However, for those *pf18pf28* axonemes in which microtubule sliding occurred, velocities doubled upon addition of the CaM-IP2 antibodies (Fig. 6 C). These velocities are significantly lower than those of *pf28* ($P < 0.001$ by *t* test). The CaM-IP2 antibodies had no effect on the sliding velocity of *pf14pf28* axonemes. These results indicate that the outer dynein arms may be one of but not the exclusive targets of regulation by the CaM complex. Therefore, we also compared dynein activity in double mutants lacking various inner dynein arm subforms.

Addition of the CaM-IP2 antibody restored dynein activity in mutant axonemes lacking the central apparatus and the I2 inner arms (*pf18ida4*; Fig. 6 D; Piperno et al., 1992), which are also known as fast protein liquid chromatography fractions a, c, and d (Kagami and Kamiya, 1992; Porter et al., 1992). The CaM-IP2 antibodies increased sliding velocities of *pf18ida4* axonemes to levels not significantly different ($P > 0.22$ by *t* test) from those of *pf18* axonemes incubated with CaM-IP2 antibody. These results suggest that the I2 inner arms are not the targets of regulation by this complex.

The *pf30* and *ida1* mutants lack the inner arm I1 or fraction f heavy chains (Piperno et al., 1990; Kagami and Kamiya, 1992; Porter et al., 1992). Addition of the CaM-IP2 antibodies to axonemes isolated from the *pf14pf30* mutant that lack the spokes and the I1 inner dynein arm failed to increase dynein activity (Fig. 6 D). These results indicate that I1 is a target for regulation by this complex. We previously reported that double mutants lacking I1 and the central apparatus (*pf18ida1*) have microtubule sliding velocities that are significantly greater than those of *pf18* axonemes ($P < 0.001$ by *t* test; Smith, 2002b). The loss of I1 from central pairless mutants partially relieves the inhibition of microtubule sliding in central apparatus–defective mutants. However, sliding velocities of *pf18ida1* are also significantly lower than those of *pf18* axonemes exposed to the CaM-IP2 antibodies ($P < 0.001$ by *t* test; Fig. 6 D). Addition of the CaM-IP2 antibodies to *pf18ida1* mutant axonemes failed to increase dynein activity to wild-type levels. These combined results support the hypothesis that the CaM-IP2, -IP3, and -IP4 complex plays a role in modulating the activity of inner dynein arm I1.

Previous studies have indicated that reduced sliding velocities in central pairless and radial spokeless mutants is correlated with the phosphorylation state of the IC138 intermediate chain of the I1 inner dynein arm (Habermacher and Sale, 1996, 1997; King and Dutcher, 1997; Yang and Sale, 2000; Hendrickson et al., 2004). Reducing the phosphorylation of IC138 using kinase inhibitors results in increased sliding velocities in these mutants (Habermacher and Sale, 1997; Yang and Sale, 2000; Smith, 2002b). Therefore, we hypothesized that addition of the CaM-IP2 antibodies to mutant axonemes may result in reduced IC138 phosphorylation and, therefore, increased dynein activity. Using antibodies generated against IC138, we performed Western blots of isolated axonemes in the presence or absence of CaM-IP2 antibodies (Fig. 7). Phosphorylated forms of IC138 have been detected on Western blots of radial spoke– and central apparatus–defective axonemes as slower migrating species that are not present when samples are treated with phosphatase (Hendrickson et al., 2004). We do not detect any decrease in the overall phosphorylation state of IC138 in either radial spokeless (*pf14*) or central pairless (*pf18*) axonemes upon the addition of anti–CaM-IP2 antibodies. These results suggest that the CaM-IP2 antibodies do not increase dynein activity by affecting the phosphorylation state of I1 IC138. Alternatively, the phosphorylation state of specific residues may be affected that cannot be detected by Western blotting.

Discussion

Our previous studies demonstrated that calcium control of motility involves the regulation of dynein-driven microtubule sliding and that CaM is a key axonemal calcium sensor (Smith, 2002a,b; Wargo et al., 2004). Using a combination of biochemical and functional approaches, we have identified a protein complex that exhibits calcium-sensitive CaM binding, localizes to

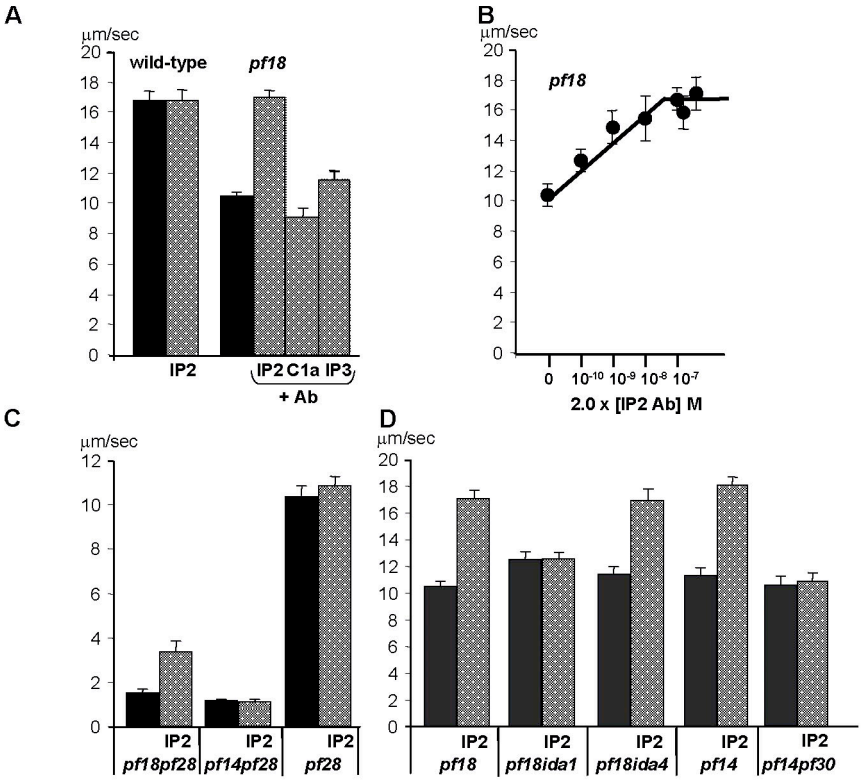

E

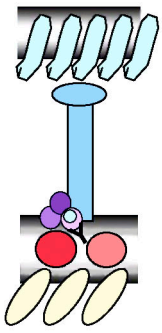

Mutant Name	Structures Lacking		Relative Velocity Anti-IP2 Antibody
wild-type	not applicable		no change
pf28	outer dynein arms		no change
pf18	central apparatus		increase
pf18pf28	central apparatus	outer dynein arms	modest increase
pf18ida4	central apparatus	inner dynein arms a,c,d	increase
pf18ida1	central apparatus	**inner dynein arm I1**	**no change**
pf14	radial spokes		increase
pf14pf28	radial spokes	outer dynein arms	no change
pf14pf30	radial spokes	**inner dynein arm I1**	**no change**

Figure 6. **CaM-IP2 modulates dynein-driven microtubule sliding.** (A) Microtubule sliding velocities of wild-type and *pf18* axonemes. The CaM-IP2 (IP2) antibodies have no effect on the sliding velocity of wild-type axonemes. In contrast, sliding velocities of *pf18* axonemes increase upon addition of the CaM-IP2 antibody. This increase is not observed in the presence of C1a-32 (C1a; Wargo et al., 2005) or CaM-IP3 (IP3) antibodies. (B) Microtubule sliding velocities of *pf18* axonemes incubated with varying concentrations of CaM-IP2 antibody. The increase in dynein activity is dose dependent, with a maximal increase in velocity at 0.2 µM CaM-IP2 antibody. (C) Microtubule sliding velocities of mutants lacking the outer dynein arms (*pf28*), outer dynein arms and the central apparatus (*pf18pf28*), and outer dynein arms and spokes (*pf14pf28*) in the presence (IP2; patterned bars) and absence (black bars) of the CaM-IP2 antibody. (D) Sliding velocities of a mutant lacking the central pair and I2 inner arm heavy chains (*pf18ida4*) increase upon the addition of anti–CaM-IP2 antibodies. Velocities of a mutant lacking the central apparatus and the I1 inner dynein arm (*pf18ida1*) are significantly higher than velocities of *pf18* ($P < 0.001$ by *t* test). However, sliding velocities of *pf18ida1* axonemes incubated with CaM-IP2 antibodies are significantly lower than those of *pf18* incubated with CaM-IP2 antibodies ($P < 0.001$ by *t* test). Sliding velocities of a radial spokeless mutant (*pf14*) increase upon the addition of anti–CaM-IP2 antibodies (IP2). However, the addition of CaM-IP2 antibodies to axonemes that lack the radial spokes and inner dynein arm I1 (*pf14pf30*) have no effect on sliding velocity. All bars represent the mean of >70 measurements ± SEM (error bars) from three or more independent experiments. (E) Summary of microtubule sliding experiments. The CaM-IP2, -IP3, and -IP4 complex (purple) is localized to the base of the spoke (blue).

the base of the radial spokes, and plays an important role in modulating dynein-driven microtubule sliding. This discovery represents an important step toward defining a molecular mechanism for control of ciliary and flagellar motility.

The identities of CaM-IP2, -IP3, and -IP4 suggest a role in regulating motility

Three polypeptides precipitated by anti-CaM antibodies form a distinct complex with CaM and were tentatively named CaM-IP2, -IP3, and -IP4. Based on the amino acid identities of these polypeptides and searches of the *C. reinhardtii* flagellar proteome, we determined that CaM-IP2, CaM-IP3, and CaM-IP4 correspond to FAP91, FAP61, and FAP251, respectively (Pazour et al., 2005). Potential mammalian homologues for each of these proteins were found in searches of sequence databases, indicating that this complex is not unique to *C. reinhardtii*. Most notably, CaM-IP2 (FAP91) is most similar to AAT-1, a protein originally identified as a testis-specific protein that interacts with AMY-1 (a c-myc–binding protein), an AKAP, and two regulatory (RII) subunits of PKA (cAMP-dependent protein kinase; Yukitake et al., 2002). Based on gel overlay assays, we have shown that CaM-IP2 binds to an AKAP (RSP3; Gaillard et al., 2001); however, none of the members of this complex appear to be AMY-1 or RII homologues. AAT-1α, a small splice variant of AAT-1, has been localized to mature sperm and appears concentrated in the sperm midpiece region (Matsuda et al., 2005). Matsuda et al. (2005) suggest that AAT-1α may be associated with mitochondria, but the precise localization of AAT-1α within sperm has not yet been determined.

In addition to AAT-1α, Matsuda et al. (2005) report the presence of several splice variants of AAT-1 expressed in various tissues, some of which have cells that possess cilia/flagella and some of which do not. The authors propose that AAT-1 may participate in additional cellular functions as well as sperm development. Northern blots of RNA isolated from *C. reinhardtii* cells before and after deflagellation reveal that *C. reinhardtii*

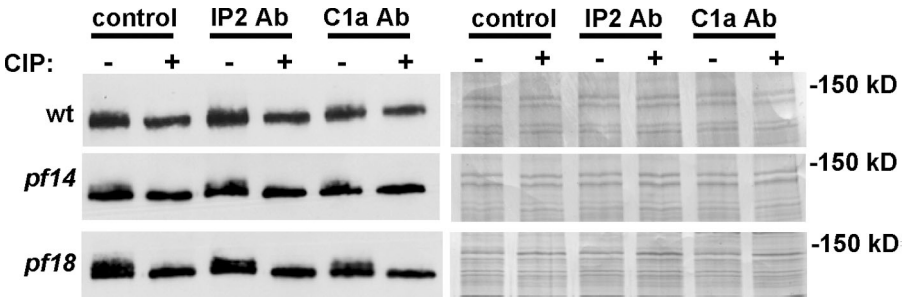

Figure 7. **Western blots of isolated axonemes (10 μg/lane) probed with antibodies generated against the I1 intermediate chain IC138.** Intermediate chain IC138, left. As indicated, some axoneme samples were treated with either anti–CaM-IP2 or anti–C1a-32 antibodies (C1a; Wargo et al., 2005) in the presence or absence of calf intestinal alkaline phosphatase (CIP). In the absence of calf intestinal alkaline phosphatase treatment, IC138 appears hyperphosphorylated in both central pairless (*pf18*) and spokeless (*pf14*) axonemes compared with wild type. No observable difference in phosphorylation is detected after the addition of CaM-IP2 antibodies. The 120–150-kD molecular mass range of Coomassie blue–stained gels of the same samples are shown as a loading control (right).

possesses a single CaM-IP2 transcript that increases in abundance after deflagellation. Therefore, in *C. reinhardtii*, CaM-IP2 is most likely present in a single isoform that primarily localizes to the flagellum. The presence of multiple splice variants of axonemal proteins in mammals, which are not observed for their *C. reinhardtii* homologues, has been previously reported (Zhang et al., 2002).

The fact that CaM-IP2 is associated with both CaM and an AKAP (RSP3) raises the intriguing possibility that this complex may play a role in integrating the calcium- and cAMP-mediated signaling pathways to produce particular changes in motility. Yukitake et al. (2002) found that mammalian AAT-1α weakly stimulated the activity of PKA and that AAT-1α itself was phosphorylated by PKA in vivo and in vitro. Although bona fide PKA homologues are not represented in the *C. reinhardtii* flagellar proteome, several AKAPS as well as proteins with domains similar to the PKA RII subunit have been identified (Gaillard et al., 2001; Yang et al., 2006). In addition, pharmacological and functional studies have implicated a role for PKA in modulating motility (Howard et al., 1994; Habermacher and Sale, 1995, 1997; Gaillard et al., 2006). We are currently investigating whether CaM-IP2 is posttranslationally modified in vivo in *C. reinhardtii*.

The presence of an NADH dehydrogenase domain in CaM-IP3 (FAP61) is suggestive of a role for this protein in energy conversion. This domain is found in oxidoreductases as well as in NADH oxidases and peroxidases. Wakabayashi and King (2006) have recently shown that in *C. reinhardtii*, motility changes that occur in response to light are altered by oxidative/reductive stress and that this effect is mediated by the redox poise of the outer dynein arms (Wakabayashi and King, 2006). Given that motility changes in response to light are generally preceded by changes in intraflagellar calcium, that CaM-IP3 is part of a complex that contains CaM, and that CaM-IP3 possesses an NADH dehydrogenase domain, one possibility is that CaM-IP3 plays a role in mediating calcium-induced changes in the flagellar redox state that affect the activity of the outer dynein arms.

CaM-IP2, -IP3, and -IP4 form a CaM- and spoke-associated complex

The conclusion that the CaM-IP2, -IP3, and -IP4 complex is associated with and localizes to the base of the radial spokes is based on the following observations. First, antibodies raised against CaM-IP2 precipitate all members of this complex as well as the radial spokes. Second, the complex cosediments with the radial spokes and spoke stalks on sucrose gradients of axonemal extracts. Finally, gel overlay assays using recombinant RSP3 reveal that RSP3 binds specifically to CaM-IP2. Previous studies have shown that mutations in RSP3 (*pf14*) result in the failure of the entire radial spoke to assemble (Huang et al., 1981) and that recombinant RSP3 binds to *pf14* axonemes (Diener et al., 1993). Therefore, RSP3 is predicted to localize to the base of the spoke and serve as a point of stalk attachment to the axonemal microtubule. Based on the clear association of the CaM-IP2, -IP3, and -IP4 complex with both CaM and the radial spokes, we propose to use the acronym CSC (CaM- and spoke-associated complex) to refer to this complex.

Given that the CSC is associated with the radial spokes in wild-type axonemal extracts, it may seem surprising that this complex was not identified in analyses of the radial spoke proteome (Yang et al., 2006). However, two important factors indicate that this complex is not part of the spoke structures. First, the *pf14* mutation results in the complete failure of the spokes to assemble; therefore, comparisons of polypeptides lacking in this mutant with those present in wild-type axonemes have historically defined radial spoke components (Huang et al., 1981; Piperno et al., 1981). Because we initially identified this complex in immunoprecipitation experiments using axonemal extracts isolated from *pf14* axonemes, its presence in this mutant would eliminate the possibility that it is part of the radial spoke structure. Second, although candidate spots possibly corresponding to these proteins are visible on the two-dimensional gels of isolated spokes by Yang et al. (2001), they are clearly present in substoichiometric amounts relative to other spoke components. Therefore, if these spots are in fact CSC components, it is possible that not every spoke is associated with a CSC. Given their presence in spokeless mutants and the fact that they may be present in substoichiometric amounts relative to spoke proteins, the CSC polypeptides do not appear to be components of the spoke structures. Experiments are currently underway to define the precise stoichiometry of this complex to radial spokes as well as their more precise localization within the axoneme.

Based on the apparent localization of the CSC to the base of the spokes, the mutant phenotype for members of this

complex might predictably include defects in radial spoke assembly. In fact, CaM-IP3 and -IP4 map to linkage group III near the *pf5* mutation, and the *pf5* mutant is defective for radial spoke assembly (Huang et al., 1981). We have sequenced the genes encoding CaM-IP3 and -IP4 from genomic DNA isolated from the *pf5* mutant and found no mutations in either gene (unpublished data). In addition, we have screened several available insertional mutant libraries for mutations in the members of this complex and found no candidate mutants. Finally, we have made numerous attempts at knocking down expression levels by RNA-mediated interference for both CaM-IP2 and -IP3 and have not obtained a stable mutant with reduced transcript levels for either gene. Therefore, the mutant phenotype for any member of this complex remains unknown.

The CSC regulates dynein-driven microtubule sliding

Using a microtubule sliding assay, we have demonstrated that the CSC plays a role in regulating dynein-driven microtubule sliding. This conclusion is based on the observation that the addition of antibodies raised against CaM-IP2 specifically restores dynein activity to axonemes that lack either the central apparatus or the radial spokes. Importantly, the increase in dynein activity is not observed upon the addition of antibodies raised against CaM-IP3 or C1a32, and the CaM-IP2 antibody effect is saturable. Therefore, the increase in dynein activity is not caused by particular buffer or rabbit serum components that may remain after affinity purification; rather, the increase in dynein activity is specific for binding of the anti–CaM-IP2 antibody.

The challenge now is to determine the mechanism by which the CSC regulates dynein activity. One possibility is that the CSC directly mediates regulatory signals from the radial spokes to the dynein arms. A second possibility is that the CSC mediates regulatory signals via the DRC. The DRC is comprised of seven polypeptides that were discovered through genetic and biochemical analyses of mutants that, when combined with central apparatus or radial spoke defect mutations, restored motility without restoring the missing structures (Huang et al., 1982; Piperno et al., 1992). The polypeptides comprising the DRC have been localized near the base of the spokes (Gardner et al., 1994; Nicastro et al., 2006). However, little is know about their identities or their function in regulating dynein (Rupp and Porter, 2003).

In these experiments, we have discovered that the two mutants that define the DRC, *pf2* and *pf3*, assemble wild-type levels of CSC components. However, only a small fraction of the CSC is associated with CaM. Our working hypothesis is that CaM association or dissociation with the CSC plays a role in modulating dynein activity. To determine whether the CSC interacts with DRC components or specific subunits of dynein arms will require the generation of additional reagents targeted to these polypeptides.

Regardless of the mechanism for CSC modulation of dynein activity, our data indicate that specific dynein subforms are affected (summarized in Fig. 6 E). Our antibodies either fail to increase dynein activity or only modestly increase dynein activity in mutants lacking the outer dynein arms. In addition, our antibodies do not increase dynein activity in double mutants lacking the I1 inner dynein arm. In contrast, the CaM-IP2 antibodies fully restore dynein activity to mutants that lack the I2 (fraction a, c, and d) inner arm heavy chains. Collectively, these results indicate that the I1 inner dynein arm as well as the outer dynein arms may be targets of regulation by the CSC.

In light of these results, it is interesting to note that in recent structural experiments, Nicastro et al. (2006) have observed a structural linkage between the inner dynein arm I1 and the outer dynein arms. In addition, work from several laboratories have indicated that inner dynein arm I1 is an important regulatory target for modulating dynein-driven microtubule sliding and that this modulation includes phosphorylation of the I1 IC138 intermediate chain (Habermacher and Sale, 1996, 1997; King and Dutcher, 1997; Yang and Sale, 2000; Hendrickson et al., 2004). Some I1-defective mutants can act as weak suppressors of paralysis for particular central apparatus–defective mutants (Porter et al., 1992). Importantly, some I1-defective mutants are deficient in their phototaxis response (King and Dutcher, 1997; Okita et al., 2005). Our results indicate that the overall phosphorylation state of IC138 does not change in either radial spokeless or central pairless mutants upon addition of the CaM-IP2 antibodies. Therefore, the increase in dynein activity we observe upon addition of our antibodies may involve a mechanism that does not alter IC138 phosphorylation. Alternatively, addition of these antibodies may ultimately result in changes in the phosphorylation of specific IC138 residues that we cannot detect by Western blotting.

An additional challenge is to determine what role the binding of Ca^{2+} to CaM plays in CSC-mediated changes in dynein activity. We have previously shown that high calcium buffer increases dynein activity in central pairless mutants but not spokeless mutants and that CaM is a key calcium sensor (Smith, 2002a). In the present study, we report the discovery of a CaM-containing complex that exhibits calcium-sensitive CaM binding. What we do not know is whether Ca^{2+}-CaM release from the CSC accounts for the increased dynein activity of central pairless mutants in high calcium conditions. Interestingly, antibodies generated against one member of this complex increase dynein activity in both central pairless and spokeless axonemes in low calcium conditions. Is there a functional relationship between antibody binding to the CSC and high calcium conditions? Our observations that the CaM-IP2 antibody increases dynein activity in mutants in which high calcium has no effect (*pf14*) suggests that the antibody acts downstream of high calcium in a signal transduction pathway. A second possibility is that high calcium affects additional axonemal targets that are missing in these mutants, and these possibilities are not mutually exclusive. For example, CaM is a component of both the central apparatus (Wargo et al., 2005) and radial spokes (Yang et al., 2001), and several calcium-binding proteins, including centrin, are associated with the dynein arms (for a complete list of both known and putative calcium-binding proteins in flagella, see Pazour et al., 2005).

To fully elucidate the mechanism by which the CSC participates in signal transduction pathways that modulate dynein activity will require precisely localizing the CSC relative to the

radial spokes and DRC, determining the stoichiometry of CSC components relative to each other and the radial spokes, identifying additional CSC interactors (potentially including polypeptides comprising the DRC or dynein arms), and determining the effects of calcium on the CSC modulation of dynein activity.

Materials and methods

C. reinhardtii strains

Strain A54-e18 (*nit1-1*, *ac17*, *sr1*, *mt+*), the wild-type strain for motility and axoneme structure, was obtained from P. Lefebvre (University of Minnesota, St Paul, MN). The central pair–defective strain *pf18*, the radial spoke–defective strains *pf17* and *pf14*, and the dynein-defective strains *pf2*, *pf3*, *ida1*, *ida4*, and *pf28* were obtained from the *C. reinhardtii* Genetics Center (Duke University). The *pf30pf28*, *pf14pf28*, and *pf14pf30* strains were obtained from W. Sale (Emory University, Atlanta, GA). Generation of the double mutants *pf18pf28* and *pf18ida1* have been previously described (Smith, 2002b). The double mutant *pf18ida4* was selected from nonparental ditype tetrads. All cells were grown in constant light in Tris acetate phosphate media (Gorman and Levine, 1965).

Preparation of flagella, flagellar extracts, and sucrose gradients

Flagella were severed from cell bodies by the dibucaine method (Witman, 1986) and isolated by differential centrifugation in NaLow (10 mM Hepes, pH 7.4, 5 mM $MgSO_4$, 1 mM DTT, 0.5 mM EDTA, and 30 mM NaCl). Axonemes were isolated by adding NP-40 (Calbiochem) to flagella for a final concentration of 0.5% (wt/vol) to remove flagellar membranes. Axonemes were initially extracted in NaHigh (10 mM Hepes, pH 7.4, 5 mM $MgSO_4$, 1 mM DTT, 0.5 mM EDTA, and 0.6 M NaCl) at a concentration of 6 mg/ml on ice for 20 min. The axonemes were pelleted, resuspended in NaHigh, and immediately pelleted again. The supernatant was discarded, and the pellet was extracted with KI (10 mM Hepes, pH 7.4, 5 mM $MgSO_4$, 1 mM DTT, 0.5 mM EDTA, 30 mM NaCl, and 0.5 M KI) at a concentration of 12 mg/ml for 30 min on ice. This extract is referred to as the KI extract or high salt extract. KI extracts were dialyzed against NaLow buffer and clarified by centrifugation at 12,000 relative centrifugal force for 10 min. For some experiments, the clarified extracts were loaded onto 5–20% sucrose gradients and subjected to ultracentrifugation at 35,000 rpm for 16 h in an SW41Ti rotor (Beckman Coulter). 0.5-ml fractions were collected from the bottom of the tube and prepared for SDS-PAGE.

Immunoprecipitation

Immunoprecipitation was performed according to Wargo et al. (2005) with the following modifications. 150 μl KI axonemal extract was incubated with ~40 μg of affinity-purified anti-CaM or anti-IP2 antibody. After four washes with $TBST_{150}$ (150 mM NaCl, 50 mM Tris-HCl, and 0.5 mM EDTA, pH 7.5), beads were resuspended in 90 μl $TBST_{150}$ and 50 μl of 5× SDS-PAGE sample buffer. For experiments performed in high calcium, a final concentration of 1 mM $CaCl_2$ was included in the $TBST_{150}$ buffer, and all washes were performed with $TBST_{150}$ + 1 mM $CaCl_2$. For immunoprecipitation performed in low calcium conditions followed by a final high calcium wash, the beads were washed as before with $TBST_{150}$, and then the beads were suspended in 100 μl $TBST_{150}$ with 2 mM $CaCl_2$. The beads were rotated for 5 min at RT and briefly spun, and the supernatant was transferred to a new tube. 100 μl $TBST_{150}$ was added to the remaining beads, and all samples were prepared for SDS-PAGE gels. For immunoprecipitation using sucrose gradient fractions, 50–80 μg of antibody was used with 1,200 μl of pooled sucrose gradient fractions. The sample was mixed for 5–8 h and washed with four 1-ml vol of $TBS\text{-}T_{150}$.

Mass spectrometry and sequence analysis

Gel bands were excised from Coomassie-stained gels. These bands were analyzed by matrix-assisted laser desorption/ionization–time of flight mass spectrometry with postsource decay conducted at the University of Massachusetts Medical School or liquid chromatography/liquid chromatography–electrospray ionization mass spectrometry performed at the Harvard Microchemistry and Proteomics Facility. Comparisons of peptide masses with translated genomic or EST sequences were made using the BLAST algorithm at the National Center for Biotechnology Information and the *Chlamydomonas* genome database (version 3.0; http://genome.jgi-psf.org/Chlre3/Chlre3.home.html). Searches of the flagellar proteome (Pazour et al., 2005) were performed using http://labs.umassmed.edu/chlamyfp/index.php.

The coding sequence for each polypeptide was confirmed by RT-PCR. RNA was isolated from wild-type *C. reinhardtii* cells before and after pH shock–induced deflagellation according to Wilkerson et al. (1994). PolyA enrichment was performed using the Oligotex mRNA kit (QIAGEN) according to the manufacturer's instructions. Reverse transcription was performed using either Superscript II or III (Invitrogen) according to the manufacturer's instructions. Subsequent PCRs were performed using primers based on the known or predicted coding regions as determined by EST, EST contig, or mass spectrometry data.

Peptide and antibody production

The CaM peptide and corresponding antibodies as well as the anti-C1a32 antibodies were generated as described previously (Wargo et al., 2005). For CaM-IP2, the first 680 bp of the coding sequence was cloned into the pET30 vector and transformed into BL21 (DE3) pLysS cells. Protein expression was induced by the addition of IPTG, and the expressed protein was purified from bacterial cell lysates using a Ni^{2+}-resin column according to the manufacturer's protocol (Novagen). For CaM-IP3 antibodies, a C-terminal peptide (CZTHAQDAVLEFARAHAAE) was synthesized and conjugated to keyhole limpet hemocyanin (Aves Labs, Inc.). For both CaM-IP2 and -IP3, polyclonal antibodies were generated in rabbits against the purified protein or peptide at Spring Valley Laboratories. Antibodies were affinity purified on Sulfolink columns (Pierce Chemical Co.) according to the manufacturer's protocol. Columns contained purified expressed protein (CaM-IP2) or purified peptide (CaM-IP3).

Gel electrophoresis, Western blots, and silver-stained gels

For immunoblots, equivalent loads of flagella (8 mg/ml), axonemes, extracts, and/or extracted axonemes were subjected to SDS-PAGE using 7% polyacrylamide gels. Gels were transferred to polyvinylidene difluoride (Immobilon P; Millipore). CaM Western blots were performed as previously described (Wargo et al., 2005). For CaM-IP2 and -IP3 Western analyses, 7% polyacrylamide gels were subject to SDS-PAGE and transferred for 1 h to polyvinylidene difluoride (Immobilon P; Millipore). Membranes were blocked for 1 h in 2% BSA (regular fraction V; A-7906; Sigma-Aldrich) in TBST (0.1% Tween and TBS, pH 7.5). For primary antibody incubations, affinity-purified anti–CaM-IP2 or anti–CaM-IP3 antibodies were diluted 1:100 or 1:5,000, respectively, and anti-RSP2 or anti-RSP3 antibodies (provided by D. Diener, Yale University, New Haven, CT) were diluted 1:5,000 in TBST. Primary antibody incubations were conducted for 2 h at RT or overnight at 4°C. Membranes were washed three times for 5 min with TBST, incubated with anti–rabbit HRP secondary antibodies (GE Healthcare), and diluted 1:30,000 in TBST. After four 5-min washes with TBST, the ECL Plus Western Blotting kit (GE Healthcare) was used for chemiluminescent detection. Gels were silver stained according to the methods described in Wargo et al. (2005).

For anti-IC138 Western blots, axonemes isolated from wild type, *pf14*, and *pf18* were resuspended at 1 mg/ml in pCa8 or pCa4 buffer containing 1 mM ATP. For some samples, 50 μg of axonemes were treated with 4 μg of affinity pure anti–CaM-IP2 or 4 μg of affinity pure anti–C1a-32 antibodies (Wargo et al., 2005). For samples that were treated with calf intestine alkaline phosphatase (Roche), the axonemes were incubated with 0.75 U of calf intestine alkaline phosphatase for 30 min at RT. 10 μg axonemal proteins were resolved on a 5% polyacrylamide gel and transferred to nitrocellulose. Blots were incubated with anti-IC138 (1:10,000 in TBST) overnight at 4°C. After washing, blots were incubated for 45 min with anti–rabbit HRP in TBST, washed, and incubated with ECL Plus for detection. The IC138 antibodies were provided by W. Sale.

Blot overlay

RSP3-GST (provided by W. Sale) was expressed and purified on a GST-resin column (Novagen) according to the manufacturer's protocol. The N terminus of CaM-IP2 was expressed and purified as described in Peptide and antibody production. For CaM-IP3, DNA sequence encoding the C-terminal 220 amino acids was cloned into pET30 and transformed into BL21 (DE3) pLysS cells. For CaM-IP4, 1.8 kb of DNA sequence encoding amino acids 1–580 was cloned into the pET30 vector. Expression was induced with IPTG, and proteins were purified from bacterial cell lysates using a Ni^{2+}-resin column (Novagen). For SDS-PAGE, 15 μg CaM-IP2 (37 kD), 15 μg CaM-IP3 (32 kD), 15 μg CaM-IP4 (62 kD), and 25 μg RSP3-GST (110 kD) were resolved on a 12% polyacrylamide gel and transferred for 40 min to nitrocellulose membrane. Membranes were blocked overnight at 4°C in 5% milk/TBST (0.1% Tween) and were incubated with 40 μg/ml RSP3-GST in 1% BSA/TBST for 2 h at RT. After three 5-min TBST washes, membranes were incubated with anti-RSP3 (1:5,000) in TBST for 1 h and with secondary antibody (anti–rabbit HRP; GE Healthcare) diluted

1:30,000 in TBST for 30 min. The ECL Plus Western Blotting kit (GE Healthcare) was used for detection.

Microtubule sliding

Flagella were severed from cell bodies by the dibucaine method (Witman, 1986) and isolated by differential centrifugation in buffer A (10 mM Hepes, pH 7.4, 5 mM $MgSO_4$, 1 mM DTT, 0.5 mM EDTA, and 50 mM potassium acetate). Axonemes were isolated by adding NP-40 (Calbiochem) to flagella for a final concentration of 0.5% (wt/vol) to remove flagellar membranes. Measurement of sliding velocity between doublet microtubules was based on the methods of Okagaki and Kamiya (1986). Microtubule sliding was initiated with buffer A containing 1 mM ATP and 2 μg/ml type VIII protease (Sigma-Aldrich) and was recorded as described previously (Smith, 2002a). All data are presented as mean ± SEM. The *t* test was used to determine the significance of differences between means. For some experiments, axonemes were incubated with affinity-purified anti–CaM-IP2 antibodies for 15 min at room temperature (22°C) before the induction of sliding. Antibody concentrations are noted on corresponding figures and are estimates based on the conversion factor of IgG = 150,000 g/mol.

Online supplemental material

Fig. S1 shows an amino acid sequence comparison of CaM-IP2 and human AAT-1. Fig. S2 shows Northern blots comparing transcript levels of CaM-IP2 and RSP3 before and after deflagellation. Fig. S3 shows Western blots of sucrose gradient fractions and immunoprecipitation experiments of corresponding pooled fractions. Online supplemental material is available at http://www.jcb.org/cgi/content/full/jcb.200703107/DC1.

We gratefully acknowledge Winfield Sale for the gift of antibodies and strains, Dennis Diener for the gift of antibodies, Heather Benson for the preparation of Fig. 4 A, and Laura Fox for technical assistance with Fig. 7.

This work was supported by National Institutes of Health grant GM66919 to E.F. Smith.

Submitted: 19 March 2007
Accepted: 3 October 2007

References

Bessen, M., R.B. Fay, and G.B. Witman. 1980. Calcium control of waveform in isolated flagellar axonemes of *Chlamydomonas*. *J. Cell Biol.* 86:446–455.

Brokaw, C.J. 1979. Calcium-induced asymmetrical beating of triton-demembranated sea urchin sperm flagella. *J. Cell Biol.* 82:401–411.

Brokaw, C.J., R. Josslin, and L. Bobrow. 1974. Calcium ion regulation of flagellar beat symmetry in reactivated sea urchin spermatozoa. *Biochem. Biophys. Res. Commun.* 58:795–800.

Diener, D.R., L.H. Ang, and J.L. Rosenbaum. 1993. Assembly of flagellar radial spoke proteins in *Chlamydomonas*: identification of the axoneme binding domain of radial spoke protein 3. *J. Cell Biol.* 123:183–190.

Gaillard, A.R., D.R. Diener, J.L. Rosenbaum, and W.S. Sale. 2001. Flagellar radial spoke protein 3 is an A-kinase anchoring protein (AKAP). *J. Cell Biol.* 153:443–448.

Gaillard, A.R., L.A. Fox, J.M. Rhea, B. Craige, and W.S. Sale. 2006. Disruption of the A-kinase anchoring domain in flagellar radial spoke protein 3 results in unregulated axonemal cAMP-dependent protein kinase activity and abnormal flagellar motility. *Mol. Biol. Cell*. 17:2626–2635.

Gardner, L.C., E. O'Toole, C.A. Perrone, T. Giddings, and M.E. Porter. 1994. Components of a "dynein regulatory complex" are located at the junction between the radial spokes and the dynein arms in *Chlamydomonas* flagella. *J. Cell Biol.* 127:1311–1325.

Gorman, D.S., and R.P. Levine. 1965. Cytochrome f and plastocyanin: their sequence in the photosynthetic electron transport chain of *Chlamydomonas reinhardtii*. *Proc. Natl. Acad. Sci. USA*. 54:1665–1669.

Habermacher, G., and W.S. Sale. 1995. Regulation of dynein-driven microtubule sliding by an axonemal kinase and phosphatase in *Chlamydomonas* flagella. *Cell Motil. Cytoskeleton*. 32:106–109.

Habermacher, G., and W.S. Sale. 1996. Regulation of flagellar dynein by an axonemal type-1 phosphatase in *Chlamydomonas*. *J. Cell Sci.* 109:1899–1907.

Habermacher, G., and W.S. Sale. 1997. Regulation of flagellar dynein by phosphorylation of a 138-kD inner arm dynein intermediate chain. *J. Cell Biol.* 136:167–176.

Hendrickson, T.W., C.A. Perrone, P. Griffin, K. Wuichet, J. Mueller, P. Yang, M.E. Porter, and W.S. Sale. 2004. IC138 is a WD-repeat dynein intermediate chain required for light chain assembly and regulation of flagellar bending. *Mol. Biol. Cell*. 15:5431–5442.

Howard, D.R., G. Habermacher, D.B. Glass, E.F. Smith, and W.S. Sale. 1994. Regulation of *Chlamydomonas* flagellar dynein by an axonemal protein kinase. *J. Cell Biol.* 127:1683–1692.

Huang, B., G. Piperno, Z. Ramanis, and D.J. Luck. 1981. Radial spokes of *Chlamydomonas* flagella: genetic analysis of assembly and function. *J. Cell Biol.* 88:80–88.

Huang, B., Z. Ramanis, and D.J. Luck. 1982. Suppressor mutations in *Chlamydomonas* reveal a regulatory mechanism for flagellar function. *Cell*. 28:115–124.

Izumi, A., and T. Miki-Noumura. 1985. Tetrahymena cell model exhibiting Ca-dependant behavior. *Cell Motil.* 5:323–331.

Kagami, O., and R. Kamiya. 1992. Translocation and rotation of microtubules caused by multiple species of *Chlamydomonas* inner-arm dynein. *J. Cell Sci.* 103:653–664.

Kamiya, R., and G.B. Witman. 1984. Submicromolar levels of calcium control the balance of beating between the two flagella in demembranated models of *Chlamydomonas*. *J. Cell Biol.* 98:97–107.

King, S.J., and S.K. Dutcher. 1997. Phosphoregulation of an inner dynein arm complex in *Chlamydomonas reinhardtii* is altered in phototactic mutant strains. *J. Cell Biol.* 136:177–191.

Matsuda, E., R. Ishizaki, T. Taira, S.M. Iguchi-Ariga, and H. Ariga. 2005. Structure and characterization of AAT-1 isoforms. *Biol. Pharm. Bull.* 28:898–901.

Naitoh, Y., and H. Kaneko. 1972. Reactivated triton-extracted models of paramecium: modification of ciliary movement by calcium ions. *Science*. 176:523–524.

Neer, E.J., C.J. Schmidt, R. Nambudripad, and T.F. Smith. 1994. The ancient regulatory-protein family of WD-repeat proteins. *Nature*. 371:297–300.

Nicastro, D., C. Schwartz, J. Pierson, R. Gaudette, M.E. Porter, and J.R. McIntosh. 2006. The molecular architecture of axonemes revealed by cryoelectron tomography. *Science*. 313:944–948.

Okagaki, T., and R. Kamiya. 1986. Microtubule sliding in mutant *Chlamydomonas* axonemes devoid of outer or inner dynein arms. *J. Cell Biol.* 103:1895–1902.

Okita, N., N. Isogai, M. Hirono, R. Kamiya, and K. Yoshimura. 2005. Phototactic activity in *Chlamydomonas* 'non-phototactic' mutants deficient in Ca2+-dependent control of flagellar dominance or in inner-arm dynein. *J. Cell Sci.* 118:529–537.

Pazour, G.J., N. Agrin, J. Leszyk, and G.B. Witman. 2005. Proteomic analysis of a eukaryotic cilium. *J. Cell Biol.* 170:103–113.

Piperno, G., B. Huang, Z. Ramanis, and D.J. Luck. 1981. Radial spokes of Chlamydomonas flagella: polypeptide composition and phosphorylation of stalk components. *J. Cell Biol.* 88:73–79.

Piperno, G., Z. Ramanis, E.F. Smith, and W.S. Sale. 1990. Three distinct inner dynein arms in *Chlamydomonas* flagella: molecular composition and location in the axoneme. *J. Cell Biol.* 110:379–389.

Piperno, G., K. Mead, and W. Shestak. 1992. The inner dynein arms I2 interact with a "dynein regulatory complex" in *Chlamydomonas* flagella. *J. Cell Biol.* 118:1455–1463.

Porter, M.E., and W.S. Sale. 2000. The 9 + 2 axoneme anchors multiple inner arm dyneins and a network of kinases and phosphatases that control motility. *J. Cell Biol.* 151:F37–F42.

Porter, M.E., J. Power, and S.K. Dutcher. 1992. Extragenic suppressors of paralyzed flagellar mutations in *Chlamydomonas reinhardtii* identify loci that alter the inner dynein arms. *J. Cell Biol.* 118:1163–1176.

Rupp, G., and M.E. Porter. 2003. A subunit of the dynein regulatory complex in *Chlamydomonas* is a homologue of a growth arrest-specific gene product. *J. Cell Biol.* 162:47–57.

Satir, P. 1985. Switching mechanisms in the control of ciliary motility. *In* Modern Cell Biology. Alan R. Liss, Inc., New York. 1–46.

Smith, E.F. 2002a. Regulation of flagellar dynein by calcium and a role for an axonemal calmodulin and calmodulin-dependent kinase. *Mol. Biol. Cell*. 13:3303–3313.

Smith, E.F. 2002b. Regulation of flagellar dynein by the axonemal central apparatus. *Cell Motil. Cytoskeleton*. 52:33–42.

Smith, E.F., and P. Yang. 2004. The radial spokes and central apparatus: mechano-chemical transducers that regulate flagellar motility. *Cell Motil. Cytoskeleton*. 57:8–17.

Verdugo, P. 1980. Ca2+-dependent hormonal stimulation of ciliary activity. *Nature*. 283:764–765.

Wakabayashi, K., and S.M. King. 2006. Modulation of *Chlamydomonas reinhardtii* flagellar motility by redox poise. *J. Cell Biol.* 173:743–754.

Wargo, M.J., and E.F. Smith. 2003. Asymmetry of the central apparatus defines the location of active microtubule sliding in *Chlamydomonas* flagella. *Proc. Natl. Acad. Sci. USA*. 100:137–142.

Wargo, M.J., M.A. McPeek, and E.F. Smith. 2004. Analysis of microtubule sliding patterns in *Chlamydomonas* flagellar axonemes reveals dynein activity on specific doublet microtubules. *J. Cell Sci.* 117:2533–2544.

Wargo, M.J., E.E. Dymek, and E.F. Smith. 2005. Calmodulin and PF6 are components of a complex that localizes to the C1 microtubule of the flagellar central apparatus. *J. Cell Sci.* 118:4655–4665.

Wilkerson, C.G., S.M. King, and G.B. Witman. 1994. Molecular analysis of the gamma heavy chain of *Chlamydomonas* flagellar outer-arm dynein. *J. Cell Sci.* 107:497–506.

Witman, G.B. 1986. Isolation of *Chlamydomonas* flagella and flagellar axonemes. *Methods Enzymol.* 134:280–290.

Yang, P., and W.S. Sale. 2000. Casein kinase I is anchored on axonemal doublet microtubules and regulates flagellar dynein phosphorylation and activity. *J. Biol. Chem.* 275:18905–18912.

Yang, P., D.R. Diener, J.L. Rosenbaum, and W.S. Sale. 2001. Localization of calmodulin and dynein light chain LC8 in flagellar radial spokes. *J. Cell Biol.* 153:1315–1326.

Yang, P., D.R. Diener, C. Yang, T. Kohno, G.J. Pazour, J.M. Dienes, N.S. Agrin, S.M. King, W.S. Sale, R. Kamiya, et al. 2006. Radial spoke proteins of *Chlamydomonas* flagella. *J. Cell Sci.* 119:1165–1174.

Yukitake, H., M. Furusawa, T. Taira, S.M. Iguchi-Ariga, and H. Ariga. 2002. AAT-1, a novel testis-specific AMY-1-binding protein, forms a quaternary complex with AMY-1, A-kinase anchor protein 84, and a regulatory subunit of cAMP-dependent protein kinase and is phosphorylated by its kinase. *J. Biol. Chem.* 277:45480–45492.

Zhang, Z., R. Sapiro, D. Kapfhamer, M. Bucan, J. Bray, V. Chennathukuzhi, P. McNamara, A. Curtis, M. Zhang, E.J. Blanchette-Mackie, and J.F. Strauss III. 2002. A sperm-associated WD repeat protein orthologous to *Chlamydomonas* PF20 associates with Spag6, the mammalian orthologue of *Chlamydomonas* PF16. *Mol. Cell. Biol.* 22:7993–8004.